

Spontaneous Arrangement of Two-way Flow in Water Bridge

Ping-Rui Tsai¹, Hong-Yue Huang¹, Cheng-Wei Lai², Yu-Ting Cheng¹,
Cheng-En Tsai², Yi-Chun Lee², Hong Hao¹, and Tzay-Ming Hong^{1*}

¹*Department of Physics, National Tsing Hua University, Hsinchu, Taiwan 30013, Republic of China*

²*Department of Chemistry, National Tsing Hua University, Hsinchu, Taiwan 30013, Republic of China and*

³*National Hsinchu Senior High School, Hsinchu, Taiwan 30013, Republic of China*

By revisiting the century-old problem of water bridge, we demonstrate that it is in fact dynamic and comprises of two coaxial water currents that carry different charges and flow in opposite directions. In the initial stage of setting up the water bridge, the inner flow is facilitated by the cone jet that is powered by H^+ and flows out of the positive-electrode beaker. A second and opposing cone jet from negative beaker is established *later* and forced to take the outer route. This spontaneous arrangement of two-way flow is revealed by using fluorescein and carbon powder as tracers, and the Particle Image Velocimetry. These two opposing flows are found to carry non-equal flux that results in a net transport of water to the negative beaker. A simple calculation based on energy conservation allows us to estimate the flow speed and cross-sectional area of these co-axial flows as a function of time and applied voltage.

Since 70.8 % of surface on earth is covered by sea, it is no wonder that scientists have shown great interest on the structure and properties of water, including extreme conditions such as water bridge (WB) at high electric field. This phenomenon [1] is realized in two beakers filled with deionized water and separated by a gap between 1~8 mm. After applying a DC voltage of about 1800 volt, a cone jet can be found to shoot from the positive beaker and establish a bridge across the gap after several attempts. This phenomenon was first reported in 1893 in a public lecture by the British engineer William Armstrong [2]. The fact that current remains less than 0.1 amp in spite of the high voltage implies a very high resistance across WB. This is why WB often becomes wiggly and eventually collapses in an hour due to heat [1]. Although there have been many hypotheses and experiments, the main mechanism behind WB and its structure remain contentious. For instance, although neutron scattering [3] and X-ray diffraction [4] all failed to find any ordered structure and settled the debate that WB might present itself as a new form of water, the experimental group on Raman effect [5] maintains that “some changes in the scattering profiles after application of the electric field are shown to have a structural origin”. Still more, the energy relaxation dynamics from infrared measurements[6] strongly indicate WB and bulk water differ at the molecular scale.

Why can WB hover in space? Fuchs [1] first ascribed this gravity-defying phenomenon to electrostatic charges on the water surface due to the high electric field and high dielectric constant of pure water. In 2009 Widom *et al.*[7] provided a detailed calculation of the WB tension in terms of the Maxwell pressure tensor in a dielectric fluid medium. In contrast, Gerald Pollack [8] speculated that the bridge is made up of a hydronium lattice or Exclusion Zone water. By taking into account the charged nature of WB, Morawetz [9] has offered a theory to calculate not only the static and dynamic stability conditions, but also details such as the creeping height, the bridge radius and length, as well as the shape of WB. Mean-

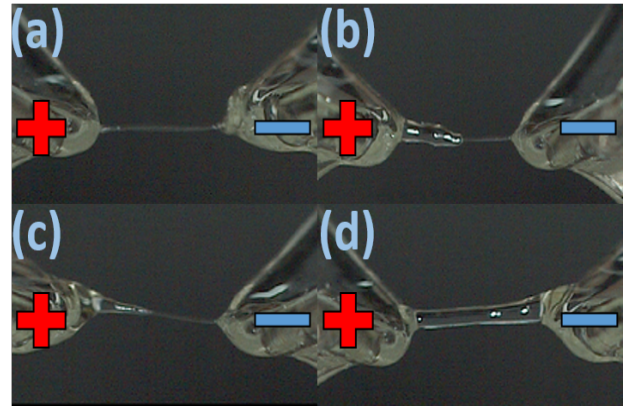


FIG. 1. (color online) (a) Cone jet shoots from the positive beaker and arrives at the negative one after several unsuccessful attempts. (b, c) Negative cone jet takes advantage of the connection in (a) and flows from negative to positive beakers by climbing on its surface. Like shovelling snow, it scrapes and causes water to pile up temporarily on the left side. (d) A thicker and more uniform WB is eventually stabilized. Videos can be found in SM I-1 of Supplemental Material (SM)[14].

while, Skinner *et al.* [4] proved in 2012 that there is no ordered structure in WB by high-energy x-ray diffraction experiments. They echoed the view by Aerov [10] that the force supporting WB is the surface tension of water, while the role of electric field \vec{E} is to avoid WB from breaking into separate drops. We are doubtful of such a proposal because WB of length 3.86 mm can be achieved at $V = 3000$ V. This is about four times longer than the maximum length of water column that can be sustained by the surface tension at $V = 0$. However, an electric field of $E = 10^6$ V/m can only increase the surface tension coefficient by 6% [11] that may be far too weak to support WB.

Let's save the debate on the origin of WB for later discussions and first concentrate on exploring the possi-

bility that a more macroscopic and yet ordered structure than the debunked crystalline one may exist. We believe the fact that the radius of H^+ ions is much smaller than that of OH^- renders the front edge of cone jet from the positive beaker being crammed with more ions and thus enjoying a stronger propulsion. By using a high-speed camera, we observe that, as soon as this cone jet [12, 13] succeeds at landing at the negative beaker as in Fig. 1(a), a surge of counter flow is observed in Fig. 1(b,c) to climb from the latter and advance on the surface of this newly-built connection. This stacking process continues until the cross section of WB stabilizes in Fig. 1(d).

One immediate question is whether this spontaneous separation of opposing flows remains true after WB is fully stabilized. To answer this question, tracers become useful at helping us visualize the flow field. Two cautions worth noting here. First, WB is sensitive and liable to ions that may accompany the addition of indicators. Second, avoid inserting the pH meter into the beaker because, like any other contact instruments, such as multimeter, electronic thermometer, and microfluidic device, it will likely crash under the high voltage. Fluorescein [15] is the first indicator we adopt to trace the direction of internal flow. Its solubility in water is merely 50 mg/L with $pK_a = 8.72$, indicating that the amount of ions generated by this compound is negligible. When added to the positive beaker, fluorescein can be seen to flow through the inner layer of WB in Fig. 2(a) and create a trail of fluorescence in the negative beaker. In contrast, the tracer occupies only the outer layer of WB when added to the negative beaker in Fig. 2(b).

As a surface tracer, carbon powders are tested in SM 1-1[14] by the capillary electrophoresis [16] to be neutral in charge before being dispersed on either beaker in Fig. 3(a). These powders are observed to travel only from negative to positive beakers. Because they always float on the water, this corroborates the picture of two-way flow established by fluorescein. According to SMI-6 [14], we measured the pH value of water and found the positive beaker becomes more alkaline with time, while the negative beaker more acidic. This leads us to conclude that the opposing flows from negative and positive beakers must be powered by OH^- and H^+ ions and take the route of outer and inner layers of WB.

In order to visualize the flow field in more detail, we appeal to Particle Image Velocimetry (PIV) that is composed of one concave lens and one cylindrical lens. Laser of 1W and 450nm passes through the optical path and illuminates the PVC particles [17] inside WB. The reflected light signal is picked up by a high speed camera with 1000~4000 fps. We perform image processing to enhance particle signals and do denoising by the Gaussian filter with the standard error 1.1. Then, Sobel edge detection is employed to determine the profile. Finally we use the Morphology to dilate the PIV image to make the particle position more discernible, as shown in SM part 3. Afterwards, pre-processing datas are converted to images via the MATLAB toolbox, PIVlab[18], for the

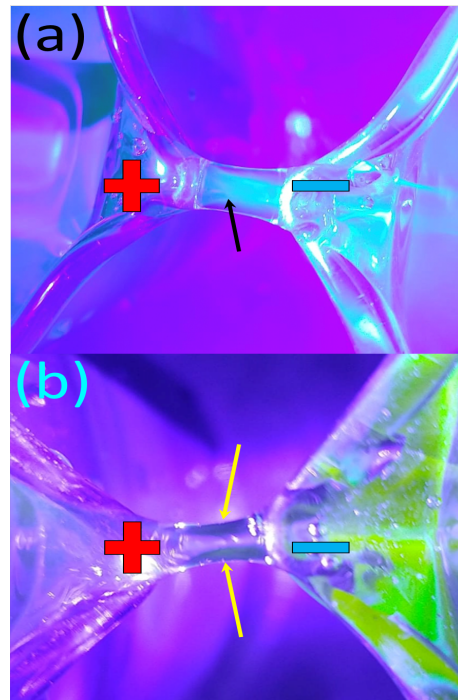


FIG. 2. (color online) Fluorescein is used to determine the direction of inner flow for WB at 10000V. A blue laser of 1W and 450nm is used to illuminate the tracer added to the positive and negative beakers in (a) and (b), respectively. The trail of fluorescein all runs toward the opposite beaker, but takes the route of inner and outer layers of WB, separately. More details can be found in SM I-2 and SM 3 [14].

analysis of flow direction[19]. A sample image is shown in Fig. 3(b) that reveals the flow vectors in the inner layer of WB mostly point towards the negative beaker. Some vortices inevitably occurred due to collisions with the opposite flow on the outer layer. To be sure, we have checked in SM 2-1 [14] that PIV particles of PVC are not affected by the high electric field. Figure 3(c) summarizes our findings of two-way flow so far. More images that were taken at different horizontal cross-sections can be found in part 3 of SM [14].

It has been reported [20] that the water level of positive beaker will fall below the negative one during the WB experiment. The growth rate of their weight difference decreases with time in Fig. 4(a, b), presumably due to the counter flow from the buildup of pressure difference in connecting pipes. The net flux of water in WB can be calculated by

$$I(V, t) = m\rho_{H_2O} \left[A_+(V, t)v_{H_2O}^+ - A_-(V, t)v_{H_2O}^- \right] \quad (1)$$

where m and ρ_{H_2O} are the molecular mass and number density of water, A_{\pm} denotes the cross-sectional area in inner and outer layers, and $v_{H_2O}^{\pm}$ are their corresponding flow speed for water [21]. A quick way to estimate $v_{H_2O}^{\pm}$ is via energy conservation, namely, the kinetic energy of

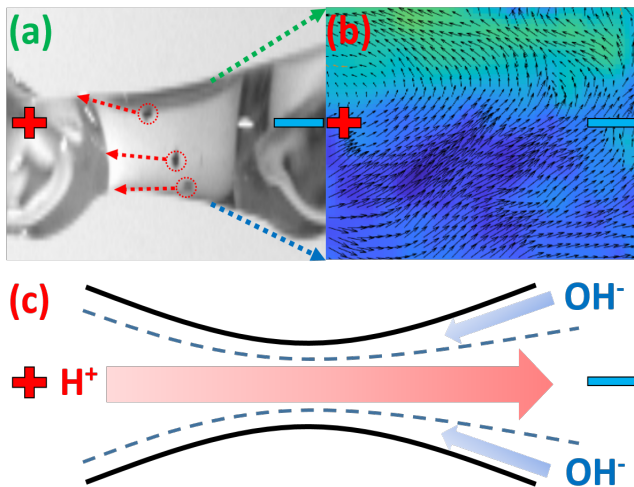


FIG. 3. (color online) Red arrows in (a) indicate that carbon powders only move from negative to positive beakers. Because they float on water, this confirms the unidirectional flow of the outer layer. The PIV image in (b) corroborates that water in the outer/inner layer on the green/blue background moves towards the positive/negative beakers. Schematic plot in (c) summarizes the arrangement of two-way flow. Clearer videos and pictures can be found in SM 1-2, SM 2-2, SM 2-3, and SM I-3 [14].

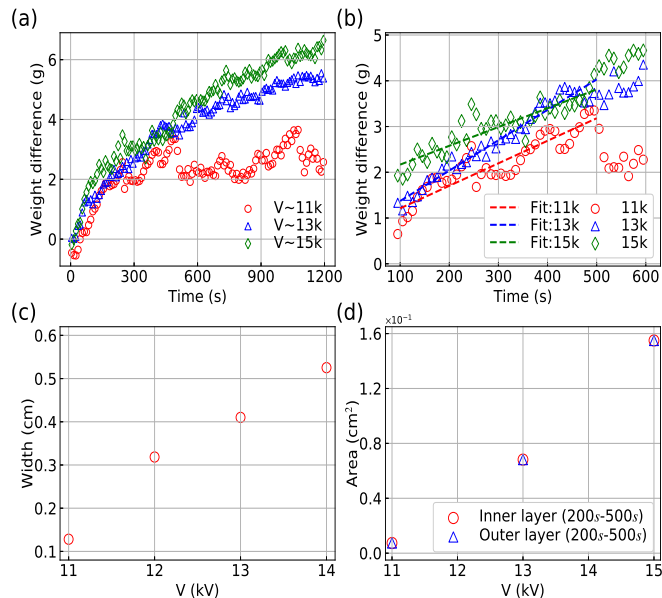


FIG. 4. (color online) The weight difference between negative and positive beakers is recorded in (a) as a function of time for three voltages. Plot (b) shows that data in (a) can be fit by a linear line during the initial 100~500 sec. The reason for using this time frame for our theoretical estimation is that WB is generally unstable before 100 sec and to avoid the complication of pressure difference built up by the principle of connecting pipes after 500 sec. In (c), the width of WB is experimentally found to increase with voltage, consistent with the trend of cross-sectional area for the inner and outer layers in (d) estimated by inputting (a) into Eq. (1).

flowing water is converted from the electrostatic energy of ion:

$$v_{H_2O}^{\pm} = \sqrt{\frac{2eV\rho_{ion}}{\epsilon m\rho_{H_2O}}} \quad (2)$$

where $e = 1.6 \times 10^{-19}$ C, the dielectric constant of liquid water is $\epsilon = 78.4$, and the number density ρ_{ion} of ions can be approximated by pH=7. By tracing the movement of carbon powders, we estimated $v_{H_2O}^{\pm}$ in the outer layer of WB with length 0.1 cm and $V=11000 \sim 15000$ V to be around 0.11 ~ 0.18 m/s, about an order of magnitude smaller than the predicted value of 1.62 ~ 1.89 m/s from Eq. (2). We believe this discrepancy comes from the creation of vortices and the fluctuation and non-uniformity for the total cross-sectional area $A_{total} \equiv A_+ + A_-$ of WB. Due to the small dimensions of WB, the effect of these unavoidable inelastic processes becomes more pronounced and renders the conversion rate from the electrostatic energy to propelling the water flow very poor - less than ~1% .

How about the energy lost to heating? For a volume of water of 3.14×10^{-9} m³ that makes up WB, the thermal loss is estimated to be about 0.131 joule for the initial 100 ~ 500 sec during which the temperature was raised by roughly 10°K. This is negligible compared to the energy input of 4000 joule from the power supply for a current of 1 mA and voltage 10000 V in the same period.

Empirically the net flux can be read off from Figs. 4(a, b) as half of their derivative. By plugging Eq.(2) into (1) and using Figs. 4(c) as an input information for A_{total} , we could estimate A_+ and A_- . As shown in Fig. 4(d), these two cross-sections increase with voltage and are comparable: $A_+/A_- \sim 1+2.00 \times 10^{-3}$, $1+2.74 \times 10^{-4}$ and $1+6.97 \times 10^{-5}$ for 11000, 13000, and 15000V.

Before concluding this work, allow us to mention another interesting experiment of ours that may contribute to clarifying the origin of WB. We are in favor of the more conventional view [22] that, since there is no bridge-like structure if water is replaced by nonpolar liquid such as n-hexane or ethanol, the potential energy $-\vec{p} \cdot \vec{E}$ between water dipoles \vec{p} and \vec{E} must play an important role. To verify this scenario, we destabilize WB by dripping extra water onto it by a burette. The excessive water is observed to hang like a drool at the bottom of WB, and eventually detach by a pinch-off at the bottleneck, as shown in Fig. 5(a). The remaining part of WB bounces back to a quasi-static height h before embarking on a much slower process of reducing back to its original shape. The relation between h and voltage is shown in Fig. 5(b). For comparison, h is strictly zero for the water column at $V = 0$ in Fig. 5(b) that is maintained solely by the surface tension. A back-of-the-envelope calculation using $mg \approx \nabla (\vec{p} \cdot \vec{E})$ gives

$$h = \sqrt{\frac{Vp}{\epsilon mg}}. \quad (3)$$

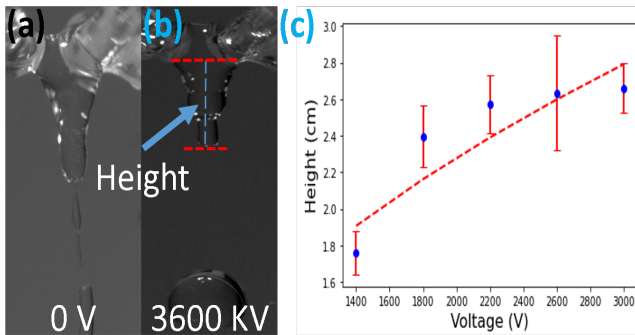


FIG. 5. (color online) In contrast to the 0.1cm-long WB at 1800 V in panel (b), the 0.05-cm water column in (a) was realized by separating two initially joined beakers at zero voltage. When extra water was poured onto both bridges, case (a) would shed off the water by one fell swoop, while (b) dividing it into several drops. Panel (c) shows how the drool height h in (b) changes with voltage. Note that case (a) does not exhibit such a quasi-static drool. More details can be found in SM I-5a, SM I-5b, and SM 4 [14].

This readily captures the concave and increasing trend of Fig. 5(c) and predicts the right magnitude for h .

In conclusion, the dynamic structure of WB is rigorously proven by experiments to comprise of two-way flow. Although this spontaneous separation into multiple layers is not new to fluid dynamics, e.g., kuroshio [23] due to different salinity and temperature, the spatial arrangement in WB is special at that it occurs in the millimeter scale. Again, unlike the example of liquid crystals[24, 25], WB involves two milli-flows that go in totally opposite directions. Microscopically water molecules in the inner layer are powered by H^+ ions that move under the high

voltage, occupies a slightly bigger cross-sectional area in WB, and flows from the positive to negative beakers. In contrast, OH^- ions drive the flow in the outer layer flows towards the opposite direction. Note that, although Ref. [9] has theoretically studied the net flux of water in WB, the author assumed the flow to be uni-directional and that the surface flow was negligible. Both assumptions contradict our observations and estimation of flow speed 10 cm/s at the outer layer from the carbon-powder experiment.

Our research did not rule out the possibility that H_3O^+ [26–28] may exist in WB. Researchers along this line of thought may want to focus on the inner flux. It will be interesting to test whether this structure of two-way flow and the imbalance between opposing fluxes also exist in other polar liquids, such as glycerin [29]. In the mean time, we suggest that a re-examination of data from x-ray diffraction and Raman spectroscopy by taking into account this complex and dynamic structure deduced by our research. Furthermore, it will be desirable to employ the technique of small-angle X-ray scattering [30, 31] on the outer layer of WB to explore possible difference in the electronic density. A potential application of this unique arrangement of two-way flow may be in the simulation of action potential of neurons that has so far relied on the equivalent circuits[32] and recent interest at studying liquid flow and control in miniaturised fluidic circuitry without solid walls[33].

We benefit from useful discussions with Jow-Tsong Shy, Sun-Ting Tsai, Li-Min Wang, and Hung-Chieh Fan Chiang, and technical supports from Yi-Shun Chang, Chun-Liang Hsieh, Zhen-Man Tian, Yen-Wen Lu and Chin-Fa Hung. Financial support by MoST in Taiwan under grants 105-2112-M007-008-MY3 and 108-2112-M007-011-MY3 is also gratefully acknowledged.

[†] These two authors contribute equally.

* ming@phys.nthu.edu.tw

- [1] E. C. Fuchs *et al.*, *J. Phys. D: Appl. Phys.* **40**, 6112 (2007).
- [2] W. G. Armstrong, *The Electrical Engineer* **10**, 154 (1893).
- [3] Elmar C. Fuchs *et al.*, *J. Phys. D: Appl. Phys.* **42**, 065502 (2009).
- [4] L. B. Skinner, C. Benmore, B. Shyam, J. K. R. Weber, and J. B. Parise, *Proc. Natl. Acad. Sci.* **109**, 16463 (2012).
- [5] R. C. Ponterio *et al.*, *J. Phys. D: Appl. Phys.* **43**, 175405 (2010).
- [6] L. Piatkowski *et al.*, *Phys. Chem. Chem. Phys.* **14**, 6160 (2012).
- [7] A. Widom, J. Swain, J. Silverberg, S. Sivasubramanian, and Y. N. Srivastava, *Phys. Rev. E* **80**, 016301 (2009).
- [8] Gerald H. Pollack, *Edgescience* **16**, 14 (2013); TED talk at <https://www.youtube.com/watch?v=i-T7tCMUDXU>
- [9] K. Morawetz, *Phys. Rev. E* **86**, 026302 (2012).
- [10] A. A. Aerov, *Phys. Rev. E* **84**, 036314 (2011).
- [11] A. Bateni, S. S. Susnar, A. W. Amirfazli, and A. W. Neumann, *Langmuir* **20**, 7589 (2004); A. Bateni, A. Amirfazli, and A. W. Neumann, *Colloids & Surfaces A: Physicochemical and Engineering Aspects* **289**, 25 (2006). How the hydrogen bonding is weakened/strengthened in the perpendicular/longitudinal direction to high electric field is studied by S. J. Suresha and A. V. Satish, *J. Chem. Phys.* **124**, 074506 (2006) and N. J. English and J. M. D. MacEnroy, *ibid.* **119**, 11806 (2003).
- [12] M. Cloupeau and B. Prunet-Foch, *J. Electrostatics* **22**, 135 (1989).
- [13] R. P. A. Hartman *et al.*, *J. Aerosol Science* **30**, 823 (1999).
- [14] See Supplemental Material at [URL] for videos, Words and a PowerPoint file.
- [15] M. C. Adams and J. Davis, *Geothermics* **20**, 53 (1991); J. R. Saylor, *Experiments in Fluids* **18**, 445 (1995); L. C. Schmued, C. Albertson, and W. Slikker, *Brain Research* **751**, 37 (1997); E. J. Noga and P. Udomkunsri, *Vet. Pathol.* **39**, 726 (2002).
- [16] J. W. Jorgenson and K. D. Lukacs, *Analytical Chemistry*

- 53**, 1298 (1981); A. J. Zemann, E. Schnell, D. Volgger, and G. K. Bonn, *Analytical Chemistry* **70**, 563 (1998).
- [17] <http://www.longwin.com/english/news/PIV-cavity-experiment-water-tunnel.html>
- [18] <https://www.mathworks.com/matlabcentral/fileexchange/27659-pivlab-particle-image-velocimetry-piv-tool>
- [19] A. K. Prasad, *Curr. Sci.* **79**, 51 (2000); K. Okamoto *et al.*, *Meas. Sci. Technol.* **11**, 685 (2000).
- [20] J. Woisetschläger, K. Gatterer, and E. C. Fuchs, *Experiments in Fluids* **48**, 121 (2009).
- [21] A list of notation for all parameters in our derivations can be found in SM [14] (SM I and SM 1-1, SM1-2, SM 2-1, SM 2-2, SM 2-3 and SM 2-4).
- [22] R. M. Namin and Z. Karimi, arXiv:1309.2222 (2013).
- [23] Sen Jan *et al.*, *Sci. Rep.* **9**, 11401 (2019).
- [24] E. I. Kats, *Low Temperature Physics* **43**, 5 (2017)
- [25] Kang Louis, *Chirality and its Spontaneous Symmetry Breaking in Two Liquid Crystal Systems* (2015). Publicly Accessible Penn Dissertations. <http://repository.upenn.edu/edissertations/1800>
- [26] J.-L. Burgot, *The Analyst* **123**, 409 (1998).
- [27] M. Tuckerman *et al.*, *J. Phys. Chem.* **99**, 5749 (1995).
- [28] L. I. Yeh *et al.*, *J. Chem. Phys.* **91**, 7319 (1989).
- [29] Álvaro G. Marín and Detlef Lohse, *Phys. Fluids* **22**, 122104 (2010).
- [30] H. D. Bale and P. W. Schmidt, *Phys. Rev. Lett.* **53**, 596 (1984).
- [31] Greg L Hura *et al.* *Nat. Methods* **6**, 606 (2009).
- [32] Sai Li *et al.*, *Nanotechnology* **28**, 31LT01 (2017).
- [33] Peter Dunne *et al.*, *Nature* **581**, 58 (2020).